

On preferential rotation of the Rattleback

Dipayan Mukherjee

Department of Mechanical Engineering, IIT Kanpur, UP - 208016, India. email: dipayanm@iitk.ac.in.

This note derives the governing equations for the rolling of the Rattleback on a flat surface. The 1-2-3 system of Euler angles is used to express the rotated body-fixed coordinate system with respect to the inertial coordinate system. The governing ordinary differential equations are derived from the Euler's laws of linear and angular momentum balance. Finally, the governing equations are solved numerically in MATLAB to demonstrate the model's prediction of spin reversal of the Rattleback.

Introduction: A Rattleback, also referred as a celt, wobblestone or a rattlestone is a semi-ellipsoidal solid object that exhibits a “preferred direction” of spin on its semi-ellipsoidal surface \mathcal{S} ; see Fig. 1a. Thus, while the Rattleback keeps on spinning if the initial spin is given in its preferred direction, a spin reversal is observed when one attempts to spin it in its non-preferred direction. Due to the complex nature of the governing differential equations of the Rattleback, an exact, closed form solution could not be attained in the earlier efforts to model the “Rattleback effect” (Walker, 1979; Caughey, 1980). Subsequently, with the availability of computers and development of efficient Runge-Kutta-type solution algorithms, researchers have reported numerical solutions to the governing equations (Kane and Levinson, 1982; Lindberg Jr and Longman, 1983; Garcia and Hubbard, 1988; Moffatt and Tokieda, 2008; Case and Jalal, 2014; Kondo and Nakanishi, 2017; Rauch-Wojciechowski and Przybylska, 2017). This note considers a practical approach towards numerically computing the response of a Rattleback under different initial conditions.

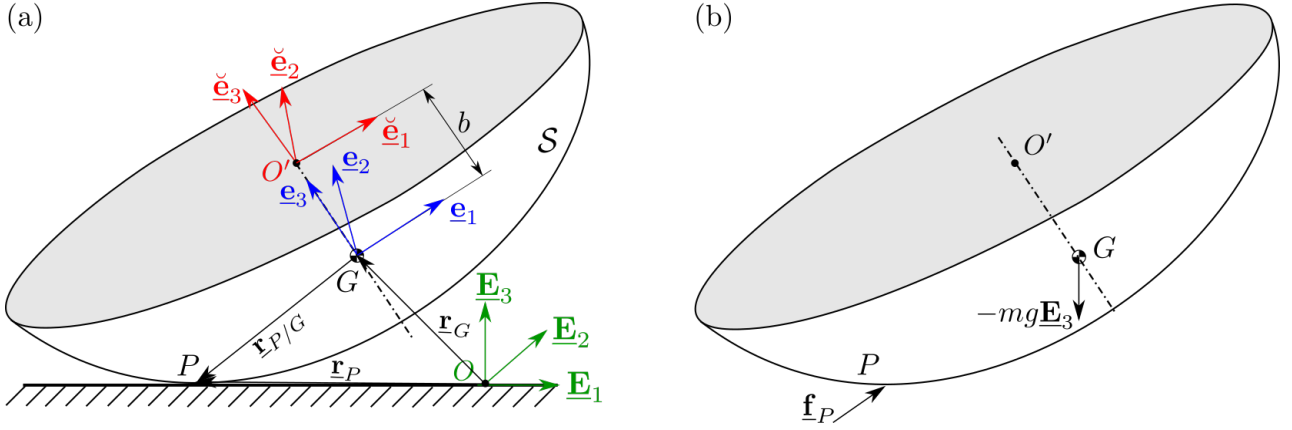


Figure 1: (a) Schematic diagram of the Rattleback having semi-ellipsoidal surface \mathcal{S} with geometrical center at O' and center of mass at G . The coordinate system $\{\underline{\mathbf{e}}_1, \underline{\mathbf{e}}_2, \underline{\mathbf{e}}_3\}$ is attached to the ellipsoid at its geometric center O' , whereas the body-fixed coordinate system $\{\underline{\mathbf{e}}_1, \underline{\mathbf{e}}_2, \underline{\mathbf{e}}_3\}$ is attached to the center of mass of the ellipsoid G . The inertial coordinate system having center at O is denoted by $\{\underline{\mathbf{E}}_1, \underline{\mathbf{E}}_2, \underline{\mathbf{E}}_3\}$. (b) Free-body-diagram of the Rattleback showing external force $\underline{\mathbf{f}}_P$ from the ground acting at point P and its weight acting along $-\underline{\mathbf{E}}_3$ at its center of mass G .

Coordinate systems and geometry: Consider the space-fixed (inertial) coordinate system (SFCS) having origin at point O on the flat surface is represented by the set $\{\underline{\mathbf{E}}_1, \underline{\mathbf{E}}_2, \underline{\mathbf{E}}_3\}$. The body-fixed coordinate system (BFCS) attached at the *geometric center* O' of the semi ellipsoid represented by $\{\underline{\mathbf{e}}_1, \underline{\mathbf{e}}_2, \underline{\mathbf{e}}_3\}$, while the BFCS attached to the center of mass G of the semi ellipsoid is denoted by $\{\underline{\mathbf{e}}_1, \underline{\mathbf{e}}_2, \underline{\mathbf{e}}_3\}$. Notice that the coordinate systems $\{\underline{\mathbf{e}}_i\}$ and $\{\underline{\mathbf{e}}_i\}$ are related by a translation along $\underline{\mathbf{e}}_3$ (or, equivalently along $-\underline{\mathbf{e}}_3$). The distance between G and O' is b , which is the depth from the cut surface of semi-ellipsoidal solid at which the center of mass is situated. The equation of surface \mathcal{S} in $\{\underline{\mathbf{e}}_i\}$ coordinate system is

$$\frac{\check{x}_1^2}{a_1^2} + \frac{\check{x}_2^2}{a_2^2} + \frac{\check{x}_3^2}{a_3^2} = 1, \quad (1)$$

where a_i ($i = 1, 2, 3$) are the principal semiaxis lengths of the ellipsoid having center at O' . Since the BFCSs $\{\underline{\mathbf{e}}_i\}$ and $\{\underline{\mathbf{e}}_i\}$ are related via a translation of length b along $\underline{\mathbf{e}}_3$, (1) can be rephrased as

$$\frac{x_1^2}{a_1^2} + \frac{x_2^2}{a_2^2} + \frac{(x_3 - b)^2}{a_3^2} - 1 := \mathcal{E}(x_1, x_2, x_3) = 0. \quad (2)$$

Since the normal to the ellipsoid at the point of contact P is always parallel to $\underline{\mathbf{E}}_3$, the position vectors x_i of P satisfy the constraint (Kane and Levinson, 1982; Garcia and Hubbard, 1988)

$$[\text{grad}(\mathcal{E})]_{\mathbf{x}_P} \times \underline{\mathbf{E}}_3 = \mathbf{0}, \quad (3)$$

where $\text{grad}(\square)$ represents gradient with respect to \mathbf{x} . Considering a representation for $\underline{\mathbf{E}}_3 = n_1^{(3)}\underline{\mathbf{e}}_1 + n_2^{(3)}\underline{\mathbf{e}}_2 + n_3^{(3)}\underline{\mathbf{e}}_3$ in the $\{\underline{\mathbf{e}}_i\}$ basis, the kinematic constraint (3) is expressed as

$$\frac{n_2^{(3)}(x_{P3} - b)}{a_3^2} - \frac{n_3^{(3)}x_{P2}}{a_2^2} = 0, \quad \frac{n_3^{(3)}x_{P1}}{a_1^2} - \frac{n_1^{(3)}(x_{P3} - b)}{a_3^2} = 0, \quad \frac{n_1^{(3)}x_{P2}}{a_2^2} - \frac{n_2^{(3)}x_{P1}}{a_1^2} = 0. \quad (4)$$

The coefficients $n_i^{(3)}$ are essentially three unknowns. However, instead of considering $n_i^{(3)}$ as primary variables, they can be conveniently expressed in terms of three *Euler angles* $\{\phi, \theta, \psi\}$. Note that x_{P1}, x_{P2} and x_{P3} also satisfy (2) since P is always on the surface \mathcal{S} . Thus, equations (4) along with (2) leads to the expression for x_i to be

$$x_{Pi} = \pm \frac{a_i^2 n_i^{(3)}}{\sqrt{\sum_{j=1}^3 (a_j n_j^{(3)})^2}} + b \delta_{i3}, \quad [\text{No sum in } i.] \quad (5)$$

where δ_{pq} is the Kronecker delta symbol. Hence, the coordinates of point P in the bases $\{\underline{\mathbf{e}}_i\}$ is determined in terms of the Euler angles and the semiaxis lengths a_i of the ellipsoid. Hence, the position of the contact point P with respect to the center of mass G is given by $\underline{\mathbf{r}}_{P/G} = x_{Pi} \underline{\mathbf{e}}_i$ (P is not a dummy index). The exact sign $(+/-)$ of x_{Pi} to be considered in (5) depends on the choice of Euler angles, which is discussed in the following.

Kinematics: The center of mass G of the Rattleback can be located at a distance $\underline{\mathbf{r}}_G$ from the inertial reference point O . Nonetheless, for describing its orientation in three dimensions it needs to define three more independent variables relating the BFCS $\{\underline{\mathbf{e}}_i\}$ to the SFCS $\{\underline{\mathbf{E}}_i\}$. Here for example, we employ a 3-1-3 system of Euler angles is employed to relate the BFCS $\{\underline{\mathbf{e}}_i\}$ to SFCS $\{\underline{\mathbf{E}}_i\}$. Thus, different intermediate coordinate systems shown in Fig. 2 are related via

$$\underline{\mathbf{E}}_i \xrightarrow{\tilde{\mathbf{R}}_1(\phi, \underline{\mathbf{E}}_1)} \underline{\mathbf{e}}'_i \xrightarrow{\tilde{\mathbf{R}}_2(\theta, \underline{\mathbf{e}}'_2)} \underline{\mathbf{e}}''_i \xrightarrow{\tilde{\mathbf{R}}_3(\psi, \underline{\mathbf{e}}''_3)} \underline{\mathbf{e}}_i, \quad (6)$$

Where $\tilde{\mathbf{R}}_1$, $\tilde{\mathbf{R}}_2$ and $\tilde{\mathbf{R}}_3$ are three rotation tensors mapping the left hand unit vectors to those in the right hand of the arrows in (6).

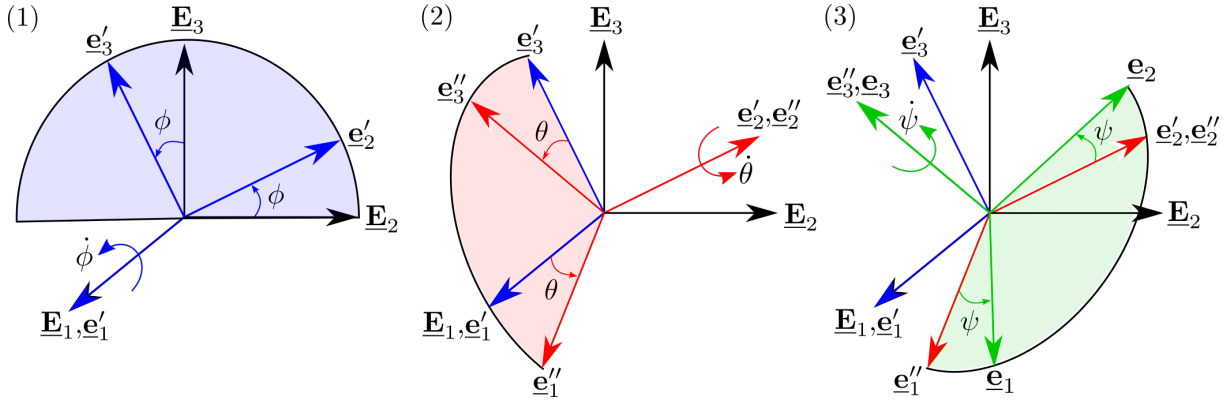


Figure 2: Sequence of rotations in a 1-2-3 system of Euler angles.

The matrix of three rotation tensors indicated in (6) expressed in their respective basis systems read

$$[\tilde{\mathbf{R}}_1]_{\underline{\mathbf{E}}} = \begin{bmatrix} 1 & 0 & 0 \\ 0 & \cos \phi & -\sin \phi \\ 0 & \sin \phi & \cos \phi \end{bmatrix}, \quad [\tilde{\mathbf{R}}_2]_{\underline{\mathbf{e}}'} = \begin{bmatrix} \cos \theta & 0 & \sin \theta \\ 0 & 1 & 0 \\ -\sin \theta & 0 & \cos \theta \end{bmatrix}, \quad [\tilde{\mathbf{R}}_3]_{\underline{\mathbf{e}}''} = \begin{bmatrix} \cos \psi & -\sin \psi & 0 \\ \sin \psi & \cos \psi & 0 \\ 0 & 0 & 1 \end{bmatrix}. \quad (7)$$

The angular velocity of the Rattleback is thus given by $\underline{\boldsymbol{\omega}} = \dot{\phi} \underline{\mathbf{E}}_1 + \dot{\theta} \underline{\mathbf{e}}'_2 + \dot{\psi} \underline{\mathbf{e}}''_3 = \dot{\phi} \underline{\mathbf{e}}'_1 + \dot{\theta} \underline{\mathbf{e}}''_2 + \dot{\psi} \underline{\mathbf{e}}_3$. Unit vectors $\underline{\mathbf{e}}'_i$ and $\underline{\mathbf{e}}''_i$ can be expressed from (6) and (7) to be

$$\{\underline{\mathbf{e}}'_i\}_{\underline{\mathbf{e}}} = [\tilde{\mathbf{R}}_3]_{\underline{\mathbf{e}}''}^T [\tilde{\mathbf{R}}_2]_{\underline{\mathbf{e}}'}^T \{\underline{\mathbf{e}}'_i\}_{\underline{\mathbf{e}}'}, \quad \{\underline{\mathbf{e}}''_i\}_{\underline{\mathbf{e}}} = [\tilde{\mathbf{R}}_3]_{\underline{\mathbf{e}}''}^T \{\underline{\mathbf{e}}''_i\}_{\underline{\mathbf{e}}''}. \quad (8)$$

Hence, the angular velocity vector $\underline{\boldsymbol{\omega}}$ expressed in the BFCS $\{\underline{\mathbf{e}}_i\}$ reads $\underline{\boldsymbol{\omega}} = \omega_i \underline{\mathbf{e}}_i$, where the components ω_i are given by

$$\omega_1 = \dot{\phi} \cos \theta \cos \psi + \dot{\theta} \sin \psi, \quad \omega_2 = -\dot{\phi} \cos \theta \sin \psi + \dot{\theta} \cos \psi, \quad \omega_3 = \dot{\phi} \sin \theta + \dot{\psi}. \quad (9)$$

We assume further the Rattleback to be *rolling without slipping* on the flat surface. Hence, the point of contact P as shown in Fig. 1a will always satisfy $\underline{\mathbf{v}}_P = \mathbf{0}$. Thus, the velocity of the center of mass G of the Rattleback is (Kane and Levinson, 1982; Lindberg Jr and Longman, 1983; Garcia and Hubbard, 1988)

$$\underline{\mathbf{v}}_G = -\underline{\boldsymbol{\omega}} \times \underline{\mathbf{r}}_{P/G}. \quad (10)$$

where $\underline{\mathbf{r}}_{P/G} = x_{Pi} \underline{\mathbf{e}}_i$ is the position vector of P with respect to G . Note that, the position vector $\underline{\mathbf{r}}_{P/G}$ changes both its length and orientation in time. Hence, the rate of change of its length needs to be taken care of in the kinematic formulation. Thus, $\dot{\underline{\mathbf{r}}}_{P/G} = \dot{x}_{Pi} \underline{\mathbf{e}}_i$. Differentiating (10) we obtain the acceleration of the center of mass $\underline{\mathbf{a}}_G$ to be

$$\underline{\mathbf{a}}_G = \dot{\underline{\mathbf{v}}}_G = -\dot{\underline{\boldsymbol{\omega}}} \times \underline{\mathbf{r}}_{P/G} - \underline{\boldsymbol{\omega}} \times (\underline{\boldsymbol{\omega}} \times \underline{\mathbf{r}}_{P/G}) - \underline{\boldsymbol{\omega}} \times \dot{\underline{\mathbf{r}}}_{P/G}. \quad (11)$$

The symbol $\overset{\circ}{\square}$ in the above equation represents the component derivative of a vector considering its unit vectors to be constant. The calculation of $\overset{\circ}{\mathbf{r}}_{P/G}$ is carried out by differentiating (5). The components of $\overset{\circ}{\mathbf{r}}_{P/G}$ are listed next. First, the time derivatives of x_{Pi} reads

$$\dot{x}_{Pi} = \pm \frac{a_i^2 \dot{n}_i^{(3)}}{\sqrt{\sum_{j=1}^3 (a_j n_j^{(3)})^2}} \mp \frac{a_i^2 n_i^{(3)}}{\left[\sum_{j=1}^3 (a_j n_j^{(3)})^2 \right]^{3/2}} \left(\sum_{j=1}^3 a_j^2 n_j^{(3)} \dot{n}_j^{(3)} \right). \quad [\text{No sum in } i] \quad (12)$$

Clearly, the essential components of \dot{x}_{Pi} are the time derivatives of the components of the unit normal vector \mathbf{E}_3 , which has components $n_1^{(3)}$, $n_2^{(3)}$ and $n_3^{(3)}$. These components can be expressed in terms of the Euler angles as $n_1^{(3)} = \sin \phi \sin \psi - \cos \phi \cos \psi \sin \theta$, $n_2^{(3)} = \cos \psi \sin \phi + \cos \phi \sin \psi \sin \theta$, and $n_3^{(3)} = \cos \phi \cos \theta$. Furthermore, $\dot{n}_i^{(3)}$ in (12) can be obtained from the relation

$$\dot{\mathbf{E}}_3 = 0, \quad (13)$$

since \mathbf{E}_3 is an unit vector that is fixed in space. Hence, $\dot{n}_i^{(3)}$ are expressed as:

$$\dot{n}_1^{(3)} = -(\omega_2 n_3^{(3)} - \omega_3 n_2^{(3)}), \quad \dot{n}_2^{(3)} = -(\omega_3 n_1^{(3)} - \omega_1 n_3^{(3)}), \quad \dot{n}_3^{(3)} = -(\omega_1 n_2^{(3)} - \omega_2 n_1^{(3)}). \quad (14)$$

Thus, substituting (9), (12) and (14) into (11), one can fully express \mathbf{a}_G in terms of the Euler angles and their first and second-order time derivatives. Finally, note that only negative signs of the terms in (5) are retained because of the term $a_i^2 n_i$ present its denominator and n_i is positive for all $0 < \{\phi, \theta, \psi\} < \frac{\pi}{2}$ for all $i = 1, 2$ and 3 . Thus, the point of contact P for $0 < \{\phi, \theta, \psi\} < \frac{\pi}{2}$ always lies in the third quadrant of the BFCS $\{\mathbf{e}_i\}$. Next, the linear and angular momentum balance laws for the Rattleback are laid down.

Kinetics: The free-body-diagram of the Rattleback is depicted in Fig. 1b. Notice that except the gravitational force acting at G , the Rattleback experiences ground reaction and frictional forces at the point of contact P . The resultant of the reaction and friction forces at P is represented by \mathbf{f}_P . Hence, the linear momentum balance law for the Rattleback reads

$$\mathbf{f}_P - mg\mathbf{E}_3 = m\mathbf{a}_G, \quad (15)$$

where m is the mass of the Rattleback and g is acceleration due to gravity. Next, the angular momentum balance for the Rattleback, written with respect to its center of mass G is expressed as

$$\mathbf{r}_{P/G} \times \mathbf{f}_P = \mathbf{I}^G \dot{\underline{\omega}} + \underline{\omega} \times \mathbf{I}^G \underline{\omega}, \quad (16)$$

where \mathbf{I}^G is the *inertia tensor* associated with the Rattleback. Substituting \mathbf{f}_P from (15) into (16) leads to

$$\mathbf{r}_{P/G} \times (mg\mathbf{E}_3 + m\mathbf{a}_G) = \mathbf{I}^G \dot{\underline{\omega}} + \underline{\omega} \times \mathbf{I}^G \underline{\omega}. \quad (17)$$

Substituting (11) and (9) into (17) one can obtain three fully coupled, second order, nonlinear ordinary differential equations (ODEs) in terms of the Euler angle triad $\{\phi, \theta, \psi\}$ and their time derivatives governing the motion of the Rattleback. Such an exercise is cumbersome and the final algebraic expressions becomes highly complicated.

An alternative way to express the governing equations as six *first order ODEs* in terms of $\dot{\phi}$, $\dot{\theta}$, $\dot{\psi}$, $\dot{\omega}_1$, $\dot{\omega}_2$, $\dot{\omega}_3$ and solving them in a computer employing the explicit Runge-Kutta-type algorithms. The first set of governing ODEs in terms of $\dot{\phi}$, $\dot{\theta}$, $\dot{\psi}$ are obtained from (9) to be

$$\begin{Bmatrix} \dot{\phi} \\ \dot{\theta} \\ \dot{\psi} \end{Bmatrix} = \begin{bmatrix} \cos \theta \cos \psi & \sin \psi & 0 \\ -\cos \theta \sin \psi & \cos \psi & 0 \\ \sin \theta & 0 & 1 \end{bmatrix}^{-1} \begin{Bmatrix} \omega_1 \\ \omega_2 \\ \omega_3 \end{Bmatrix} \equiv \begin{Bmatrix} \dot{\phi} \\ \dot{\theta} \\ \dot{\psi} \end{Bmatrix} = [\mathbf{\Phi}]^{-1} \begin{Bmatrix} \omega_1 \\ \omega_2 \\ \omega_3 \end{Bmatrix}. \quad (18)$$

Next, the angular momentum balance law (17) leads to three set of ODEs in terms of $\dot{\omega}_1$, $\dot{\omega}_2$, $\dot{\omega}_3$. First substitute \mathbf{a}_G from (11) into (17) to obtain

$$\mathbf{r}_{P/G} \times [mg\mathbf{E}_3 - m\dot{\underline{\omega}} \times \mathbf{r}_{P/G} - m\underline{\omega} \times (\underline{\omega} \times \mathbf{r}_{P/G}) - m\underline{\omega} \times \overset{\circ}{\mathbf{r}}_{P/G}] = \mathbf{I}^G \dot{\underline{\omega}} + \underline{\omega} \times \mathbf{I}^G \underline{\omega}. \quad (19)$$

Rearranging terms in (19) yields:

$$mg(\mathbf{r}_{P/G} \times \mathbf{E}_3) - m\mathbf{r}_{P/G} \times [\underline{\omega} \times (\underline{\omega} \times \mathbf{r}_{P/G})] - m\mathbf{r}_{P/G} \times (\underline{\omega} \times \overset{\circ}{\mathbf{r}}_{P/G}) - \underline{\omega} \times \mathbf{I}^G \underline{\omega} = \mathbf{I}^G \dot{\underline{\omega}} - m\mathbf{r}_{P/G} \times (\mathbf{r}_{P/G} \times \dot{\underline{\omega}}). \quad (20)$$

The last equation can be rephrased in tensor notations as

$$mg\mathbf{X}\mathbf{E}_3 - m\mathbf{X}\mathbf{W}^2\mathbf{r}_{P/G} - m\mathbf{X}\mathbf{W}\overset{\circ}{\mathbf{r}}_{P/G} - \mathbf{W}\mathbf{I}^G\mathbf{W} = [\mathbf{I}^G - m\mathbf{X}^2]\dot{\underline{\omega}}, \quad (21)$$

where \mathbf{X} and \mathbf{W} are skew-symmetric tensors, whose axial vectors are $\mathbf{r}_{P/G}$ and $\underline{\omega}$, respectively. Hence, the matrices of \mathbf{X} and \mathbf{W} in the BFCs \mathbf{e}_i read

$$[\mathbf{X}]_{\mathbf{e}} = \begin{bmatrix} 0 & -x_{P3} & x_{P2} \\ x_{P3} & 0 & -x_{P1} \\ -x_{P2} & x_{P1} & 0 \end{bmatrix}, \quad \text{and} \quad [\mathbf{W}]_{\mathbf{e}} = \begin{bmatrix} 0 & -\omega_3 & \omega_2 \\ \omega_3 & 0 & -\omega_1 \\ -\omega_2 & \omega_1 & 0 \end{bmatrix}. \quad (22)$$

Finally, one can express the vector equation (21) in matrix form as

$$\{\dot{\underline{\omega}}\}_{\mathbf{e}} = [\mathbf{I}^R]_{\mathbf{e}}^{-1} \{\mathbf{b}\}_{\mathbf{e}}, \quad (23)$$

where $\mathbf{I}^R = \mathbf{I}^G - m\mathbf{X}^2$ and $\mathbf{b} = mg\mathbf{X}\mathbf{E}_3 - m\mathbf{X}\mathbf{W}^2\mathbf{r}_{P/G} - m\mathbf{X}\mathbf{W}\mathbf{r}_{P/G} - \mathbf{W}\mathbf{I}^G\underline{\omega}$. Hence, we finally obtain the six set of six ODEs (18) and (23) in terms of six variables $\phi, \theta, \psi, \tilde{\omega}_1, \omega_2$ and $\tilde{\omega}_3$. Note that the degree-of-freedom is three since all three ω_i can be expressed as functions of the angles and their time derivatives and hence, one can, in principle, obtain three second order ODEs from (23). Nevertheless, to simplify the algebra and to facilitate numerical solutions of the governing ODEs, we have considered ω_1, ω_2 and ω_3 to be three additional independent variables with three more governing equations given by (18). Next, we specify physical parameters associated with the Rattleback and perform computations for its motion.

Results: The physical parameters for the Rattleback are obtained from Kane and Levinson (1982) and the computations are performed via employing the classical 4th order Runge-Kutta-based solver `ode45` of MATLAB. The mass and physical dimensions of the Rattleback are taken to be $m = 1\text{kg}$, $a_1 = 20\text{cm}$, $a_2 = 3\text{cm}$, $a_3 = 2\text{cm}$ and $b = 0.5\text{cm}$. The matrix of the inertia tensor \mathbf{I}^G in the principle coordinate system \mathbf{e}_i is expressed as

$$[\mathbf{I}^G]_{\mathbf{e}} = \begin{bmatrix} 2.0 & -0.5 & 0 \\ -0.5 & 16.0 & 0 \\ 0 & 0 & 17.5 \end{bmatrix} \text{ Kg} \cdot \text{cm}^2. \quad (24)$$

The first set of simulations are performed to demonstrate the preferential rotation of Rattlebacks. For instance, the first set of numerical computations consider the initial conditions to be $\phi = \theta = \psi = 10^{-6}$ rad, $\omega_1 = \omega_2 = 0$, while $\omega_3 = \omega_0$ and $\omega_3 = -\omega_0$ rad s⁻¹. Results shown for the temporal evolutions of ω_1, ω_2 and ω_3 are shown in Fig. 3 for two initial angular velocities $\omega_0 = 2.5$ and 5.0 rad s⁻¹.

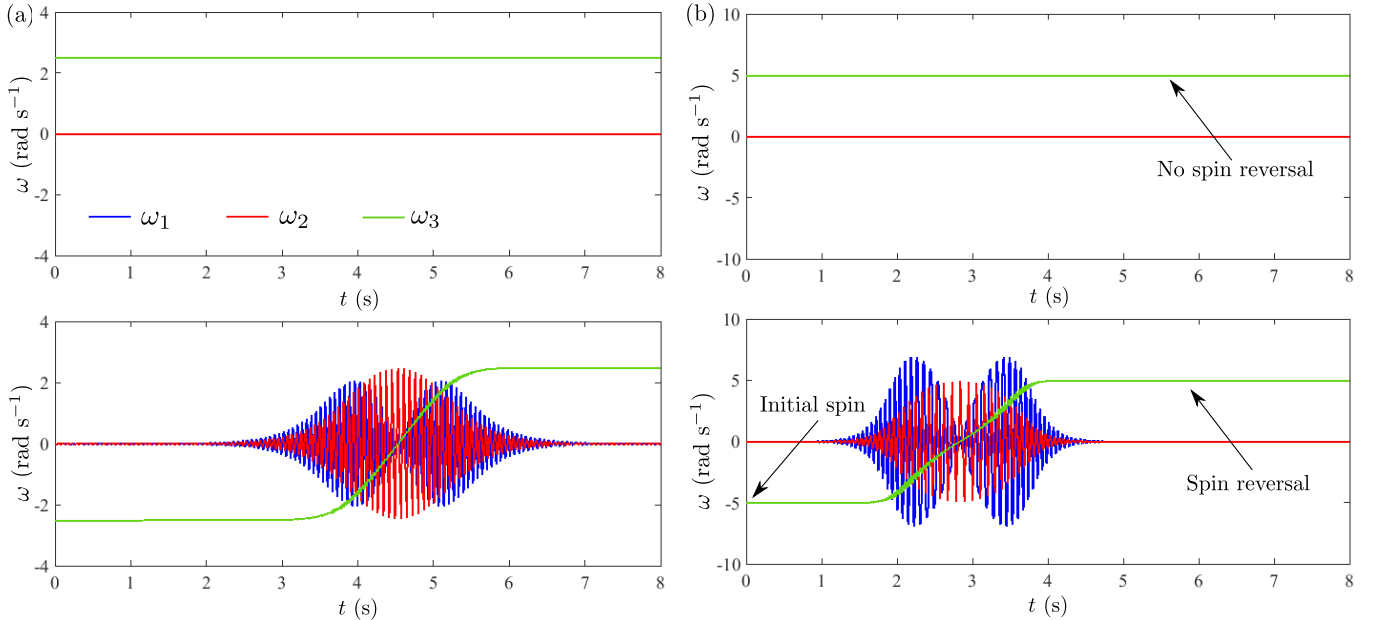


Figure 3: Evolution of ω_1, ω_2 and ω_3 in time for (a) $\omega_0 = 2.5$ rad s⁻¹ and (b) 5.0 rad s⁻¹. Top figures, where initial spin was given counter clockwise about \mathbf{E}_3 , show no spin reversal. Spin reversal is observed for clockwise initial spin cases accompanied by high frequency oscillations about \mathbf{e}_1 and \mathbf{e}_2 during the reversal.

The results match quantitatively with that of Kane and Levinson (1982) and qualitative match with all the above-cited articles are observed. It is observed from Fig. 3 that a higher initial spin in the "non-preferred" direction will delay the spin reversal of the Rattleback, while no spin reversal is observed when the initial spin is given along the "preferred" direction of the Rattleback. Moreover, the initial spin energy is transferred to the energy of oscillation of the Rattleback about the \mathbf{e}_1 and \mathbf{e}_2 axes of the BFCs during the reversal of its spin. Thus, high frequency oscillations about \mathbf{e}_1 and \mathbf{e}_2 are observed at the time of spin reversal as referred by "rattling up and down" by Walker (1979).

Nonetheless, once the reversal is complete, the spin energy becomes equal to the initially supplied one, but now having the Rattleback spinning along its preferred direction.

A second feature observed in the Rattleback is its spin initiated by an initial tapping. If the semi-ellipsoidal solid is tapped on one side of its face and released, it is observed to be rattling up and down initially, followed by a spin in its preferred direction. The model also predicts this feature of the Rattleback as shown in the results in Fig. 4. The

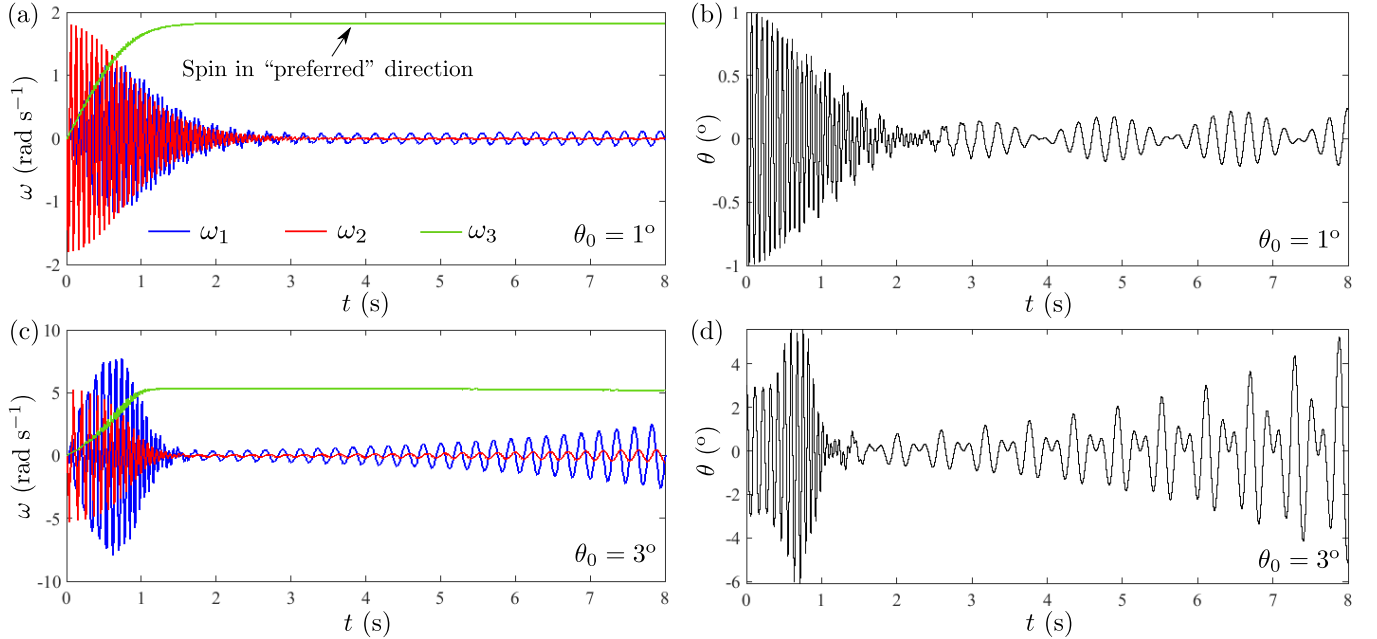


Figure 4: Time evolution of ω_1 , ω_2 and ω_3 in time for (a) $\theta_0 = 1^\circ$ and (c) $\theta_0 = 3^\circ$. Variation of angle θ in time for (b) $\theta_0 = 1^\circ$ and (d) $\theta_0 = 3^\circ$. No initial spin is applied.

initial conditions for this set of computations are taken to be $\omega_1 = \omega_2 = \omega_3 = 0$, $\phi = \psi = 10^{-6}$ and $\theta = \theta_0$. Two set of computations are shown in Fig. 4, where it is observed that the earlier “rattling” effect in the Rattleback vanishes soon after the initial tapping and subsequently, it starts spinning its preferred direction; see Fig. 4a and c. Moreover, it is observed that the spin rate is greater if the initial tapping angle is more. Temporal evolution of the angle $\theta(t)$ shown in Fig. 4b and d also confirms these observations.

Remarks on the choice of Euler angles: The key features of Rattleback’s motion are its spin reversal and its “rattling” up and down during the spin reversal. Hence, periodic oscillations around $\theta = 0$ are expected during such a motion. Thus, the sequence of Euler angles should be chosen so that the matrix $[\tilde{\Phi}]$ is non-singular for $\theta = 0$. One can note that the $[\tilde{\Phi}]$ written in (18) is not singular for $\theta = 0$ for the 1-2-3 sequence of Euler angles. However, one can verify that the commonly used 3-1-3 Euler angles would lead to a singular $[\tilde{\Phi}]$ at $\theta = 0$. The choice of 1-2-3 sequence in the present case is heuristic and can be suitably replaced by any other sequence given $[\tilde{\Phi}]$ is non-singular at $\theta = 0$. The choice of Euler angles should be made considering the geometry of the problem and possible range of θ in the solutions to avoid any singularity-related numerical issues in the computations.

References

- W Case and S Jalal. The rattleback revisited. *American Journal of Physics*, 82(7):654–658, 2014.
- TK Caughey. A mathematical model of the “rattleback”. *International Journal of Non-Linear Mechanics*, 15(4-5):293–302, 1980.
- A Garcia and M Hubbard. Spin reversal of the rattleback: theory and experiment. *Proceedings of the Royal Society of London. A. Mathematical and Physical Sciences*, 418(1854):165–197, 1988.
- TR Kane and DA Levinson. Realistic mathematical modeling of the rattleback. *International Journal of Non-Linear Mechanics*, 17(3): 175–186, 1982.
- Y Kondo and H Nakanishi. Rattleback dynamics and its reversal time of rotation. *Physical Review E*, 95(6):062207, 2017.
- RE Lindberg Jr and RW Longman. On the dynamic behavior of the wobblestone. *Acta mechanica*, 49(1-2):81–94, 1983.
- HK Moffatt and T Tokieda. Celt reversals: a prototype of chiral dynamics. *Proceedings of the Royal Society of Edinburgh Section A: Mathematics*, 138(2):361–368, 2008.
- S Rauch-Wojciechowski and M Przybylska. Understanding reversals of a rattleback. *Regular and Chaotic Dynamics*, 22:368–385, 2017.
- J Walker. The mysterious “rattleback”: a stone that spins in one direction and then reverses (the amateur scientist). *Scientific American*, pages 144–149, 1979.

Appendix: Matlab code

```

1  % -----
2  function z = rattleback_simulator_123H()
3  clear all
4  % Define parameters -----
5  % -----
6  m=1; % Mass of Rattleback
7  g = 9.81; % Accn due to gravity
8  a1 = 0.2; % Semi-major axis length of the Rattleback
9  a2 = 0.03; % Semi-minor axis 1
10 a3 = 0.02; % Semi-minor axis 2
11 b = 0.005; % Position of CM below the geometric center of the ellipsoid
12 Ixx = 0.0002; % Mass moment of inertia about e1
13 Iyy = 0.0016; % Mass moment of inertia about e2
14 Izz = 0.00175; % Mass moment of inertia about e3
15 Ixy = -0.00005; % Product of inertia
16 %Ixy = 0.0; % Product of inertia
17 % -----
18 param_vec = [m g a1 a2 a3 b Ixx Iyy Izz Ixy];
19 % -----
20 t = linspace(0,8,250000); % Time span of simulation
21 options = odeset('AbsTol',1e-12,'RelTol',1e-12);
22 % Call ODE45 to solve 6 set of simultaneous ODEs
23 % -----
24 [T,Y] = ode45(@(t, y) equns123(t, y, param_vec),t, [0,0,5,1.0e-6,1.0e-6,1.0e-6],
    options);
25 % -----
26 y=Y(:,1:6); % Output variables
27 omega11=Y(:,1);
28 omega12=Y(:,2);
29 omega13=Y(:,3);
30 phi1=Y(:,4)*180/pi;
31 theta1=Y(:,5)*180/pi;
32 psi1=Y(:,6)*180/pi;
33 % -----
34 [T,Y] = ode45(@(t, y) equns123(t, y, param_vec),t, [0,0,-5,1.0e-6,1.0e-6,1.0e-6],
    options);
35 % -----
36 phi2=Y(:,4)*180/pi;
37 theta2=Y(:,5)*180/pi;
38 psi2=Y(:,6)*180/pi;
39 omega21=Y(:,1);
40 omega22=Y(:,2);
41 omega23=Y(:,3);
42 % -----
43 plottingfn(T,omega11,omega12,omega13,omega21,omega22,omega23,theta1,theta2)
44 %animate(phi1,theta1,psi1,phi2,theta2,psi2)
45 end
46
47 % -----
48 % Set of first order ODEs -----
49 % -----
50
51 function dy = equns123(t, y, param_vec)
52
53 m=param_vec(1);
54 g = param_vec(2);
55 a1 = param_vec(3);
56 a2 = param_vec(4);
57 a3 = param_vec(5);

```

```

58 b = param_vec(6);
59 Ix = param_vec(7);
60 Iy = param_vec(8);
61 Iz = param_vec(9);
62 Ixy = param_vec(10);
63
64 Iten = [Ix Ixy 0; Ixy Iy 0; 0 0 Iz]; % Moment of inertia tensor -----
65
66 w1=y(1);
67 w2=y(2);
68 w3=y(3);
69 phi=y(4);
70 theta=y(5);
71 psi=y(6);
72
73 % Define n1, n2, n3 in terms of the Euler angles -----
74 n1 = sin(phi)*sin(psi)-cos(psi)*sin(theta)*cos(phi);
75 n2 = cos(psi)*sin(phi)+sin(psi)*sin(theta)*cos(phi);
76 n3 = cos(theta)*cos(phi);
77
78 % Define xp1, xp2, xp3 in terms of n1, n2, n3 and geometric parameters ----
79 sum_ajnj = a1^2*n1^2+a2^2*n2^2+a3^2*n3^2;
80 xp1 = -a1^2*n1/sqrt(sum_ajnj);
81 xp2 = -a2^2*n2/sqrt(sum_ajnj);
82 xp3 = -a3^2*n3/sqrt(sum_ajnj)+b;
83
84 % Calculate n1_dot, n2_dot, n3_dot -----
85 n1d = -(w2*n3-w3*n2);
86 n2d = -(w3*n1-w1*n3);
87 n3d = -(w1*n2-w2*n1);
88
89 % Calculate xp1_dot, xp2_dot, xp3_dot
90 sum_ajnj_dot = a1^2*n1*n1d+a2^2*n2*n2d+a3^2*n3*n3d;
91 xp1d = -(a1^2*n1d/sqrt(sum_ajnj)-a1^2*n1/(sum_ajnj)^1.5*(sum_ajnj_dot));
92 xp2d = -(a2^2*n2d/sqrt(sum_ajnj)-a2^2*n2/(sum_ajnj)^1.5*(sum_ajnj_dot));
93 xp3d = -(a3^2*n3d/sqrt(sum_ajnj)-a3^2*n3/(sum_ajnj)^1.5*(sum_ajnj_dot));
94
95 % Define skew symmetric matrices
96 Wm = [0 -w3 w2; w3 0 -w1; -w2 w1 0];
97 Xm = [0 -xp3 xp2; xp3 0 -xp1; -xp2 xp1 0];
98 % Define column vectors
99 Rv = [xp1; xp2; xp3];
100 Rdv = [xp1d; xp2d; xp3d];
101 E3v = [n1; n2; n3];
102 Wv = [w1; w2; w3];
103
104 % Calculate Ir
105 Ir = Iten - m.*Xm*Xm;
106 % Calculate the RHS vector in the angular momentum balance -----
107 rhsvc = -Wm*Iten*Wv-m.*Xm*(Wm*(Wm*Rv))-m.*Xm*(Wm*Rdv)+m*g.*(Xm*E3v);
108
109 % Calculation of omega_dot vector -----
110 omegad = inv(Ir)*rhsvc;
111
112 %
113 % Input the computed omega dot to the function output dy
114 dy(1) = omegad(1);
115 dy(2) = omegad(2);
116 dy(3) = omegad(3);
117
118 %

```

```

119 % Calculation of {phi_dot, theta_dot, psi_dot} vector -----
120 Phim = [cos(theta)*cos(psi) sin(psi) 0;
121 -cos(theta)*sin(psi) cos(psi) 0;
122 sin(theta)          0      1];
123
124 angd = inv(Phim)*Wv;
125
126 dy(4) = angd(1);
127 dy(5) = angd(2);
128 dy(6) = angd(3);
129
130 dy = dy(:);
131 end
132
133 %
134 % -----
135 % Plot -----
136 % -----
137
138 function z=plottingfn(T,omega11,omega12,omega13,omega21,omega22,omega23,theta1,
    theta2)
139 subplot(2,1,1)
140 plot(T,omega11,'b-')
141 hold on
142 plot(T,omega12,'r-')
143 plot(T,omega13,'g-')
144 hold off
145 legend({'$\omega_1$', '$\omega_2$', '$\omega_3$'},Interpreter='latex');
146 xlabel('$t$ (s)',Interpreter='Latex');
147 ylabel('$\omega$ (rad/s)',Interpreter='Latex');
148
149 subplot(2,1,2)
150 plot(T,omega21,'b-')
151 hold on
152 plot(T,omega22,'r-')
153 plot(T,omega23,'g-')
154 hold off
155 legend({'$\omega_1$', '$\omega_2$', '$\omega_3$'},Interpreter='latex');
156 xlabel('$t$ (s)',Interpreter='Latex');
157 ylabel('$\omega$ (rad/s)',Interpreter='Latex');
158
159
160 figure
161 subplot(2,1,1)
162 plot(T,theta1,'b-')
163 ylim([-5 5])
164 xlabel('$t$ (s)',Interpreter='Latex');
165 ylabel('$\theta^{\circ}$',Interpreter='Latex');
166
167 subplot(2,1,2)
168 plot(T,theta2,'b-')
169 xlabel('$t$ (s)',Interpreter='Latex');
170 ylabel('$\theta^{\circ}$',Interpreter='Latex');
171
172
173 end

```